

Materials and Physics of High Temperature Superconductors:
A Summary, Two Recent Experiments and a Comment

C. W. Chu

Department of Physics and Texas Center for Superconductivity, University of Houston,
202 Houston Science Center, Houston, Texas 77204-5002; Lawrence Berkeley National
Laboratory, 1 Cyclotron Road, Berkeley, California 94720; and Hong Kong University
of Science and Technology, Hong Kong

e-mail: cwchu@uh.edu

ABSTRACT

After the extensive worldwide research of the last 15 years, great progress has been made in all areas of high temperature superconductivity, namely, materials, science, and technology. In this presentation, I shall first summarize what we know and do not know about the materials and physics, but only of the cuprate high temperature superconductors because of their higher transition temperatures, and describe the material challenges encountered in unraveling the mystery of superconductivity in this class of materials. I shall then present results of two recent interesting experiments concerning the propositions of the possible co-existence of superconductivity and ferromagnetism in cuprates, and the possible existence of high temperature superconductivity in multi-wall carbon nanotubes, respectively. Finally, I shall briefly comment on the recent reports of exciting results for field-induced superconductivity.

Journal: Physica Scripta
Date: January 29, 2002
PACS Nos.: 74.72.-h, 74.70.Wz, 74.90.+n

1. Cuprate High Temperature Superconductors

Many review articles [1] on cuprate high temperature superconductors are available. In this section of the paper, I will summarize some simple facts about this compound system and some questions I consider unresolved. Therefore, only a few references are given. For more references, one may refer to the review articles.

1.1 Some Statistics:

- There have been more than 150 high temperature superconducting non-intermetallic compounds discovered with a transition temperature (T_c) higher than 23.2 K, the record of superconducting intermetallic compounds prior to the recent discovery of MgB_2 . They fall into the material systems of cuprates [2], bismuthates [2], fullerites [3], and field-induced surface superconductors [4].
- Only cuprates and field-induced surface superconductors have a $T_c > 77$ K, the liquid nitrogen boiling temperature, with superconductivity occurring in the bulk in the former, whereas only in the first molecular layer of the latter.

- As shown in Fig. 1, T_c has risen steadily to the present records of 134 K [5] and 164 K [6] in $\text{HgBa}_2\text{Ca}_2\text{Cu}_3\text{O}_{8+\delta}$ at ambient pressure and under ~ 30 GPa, respectively. These temperatures are achievable by household air-conditioning technology or in the cargo-bay of the Space Shuttle when the proper steps are taken. While no higher T_c 's have been attained since 1993, several new high temperature superconducting compound systems have been discovered since then, *e.g.* $\text{Ba}_2\text{Ca}_{3-y}\text{Cu}_{3+y}\text{O}_x$ with a T_c up to 126 K [7], MgB_2 with a T_c of 40 K [8], and field-induced surface superconductivity with a T_c up to 117 K in intercalated C_{60} [9] and 89 K in CaCuO_2 [10]. Superconductivity has also been reported in uncoupled single-wall carbon nanotubes with a mean-field transition temperature up to 15 K [11].
- The carrier density is $\sim 10^{21}/\text{cc}$, almost two orders of magnitude smaller than that of the conventional low temperature superconductors. The coherence length of the cuprates is also relatively short in comparison with the low temperature superconductors, *i.e.* ~ 3 Å perpendicular to the CuO_2 -plane and ~ 10 Å along the plane, and both are smaller than or comparable to the lattice parameters of the cuprates.

- The upper critical field (H_{c2}) has reached ~ 150 T perpendicular to the CuO_2 plane in cuprates at 0 K, a million times the earth's magnetic field. In principle, an ultra-high-field electromagnet and, thus, a powerful compact accelerator can be built.
- Critical current densities (J_c) obtained in self-field at 77 K are: $\sim 5 \times 10^6$ A/cm² in $\text{YBa}_2\text{Cu}_3\text{O}_7$ (YBCO) thin films; $\sim 10^6$ A/cm² in YBCO thick films on single-crystalline and flexible substrates; and $\sim 10^5$ A/cm² in YBCO bulk or $\text{Bi}_2\text{Sr}_2\text{Ca}_2\text{Cu}_3\text{O}_{10}$ (BSCCO) tapes. At 77 K, J_c decreases rapidly with an externally applied magnetic field for BSCCO but much less so for YBCO. However, at 4.2 K, both YBCO and BSCCO outperform the best conventional superconductor Nb_3Sn at fields above 15 T. Prototype high temperature superconducting power transmission lines, transformers and motors have been built and are being demonstrated, and thin film devices for magnetocardiography, magnetic resonance imaging, and other uses have been fabricated and tested successfully.
- The microwave surface impedance at 77 K has reached that of the conventional superconductor Nb but at a much lower temperature of 7.7 K, orders of magnitude smaller than Cu at 77 K below 10 GHz. Hundreds of prototype base stations using high temperature superconducting filters for cell-phone communication have been constructed and successfully field-tested.

1.2 Major Observations:

- As shown schematically in Fig. 2, all cuprate high temperature superconductors have a perovskite-like layer structure. In spite of the large number of compounds, they can be represented by the generic formula $A_m E_2 R_{n-1} Cu_n O_{2n+m+n}$, where A, E, and R are various cations, often with E = Ba, Sr, or Ca, and R = Ca or a rare-earth element. They can be designated simply by $A_m 2(n-1)n$ or, when A is absent, by $02(n-1)n$. $A_m E_2 R_{n-1} Cu_n O_{2n+m+n}$ can also be written as $[(EO)(AO)_m(EO)]\{(CuO_2)[R(CuO_2)]_{n-1}\}$, representing a stacking sequence of m (AO)-layers inserted between 2 (EO)-layers on top of n (CuO_2)-layers interleaved by (n-1) R-layers. As a result, n depicts the number of (CuO_2)-layers per unit formula. The (AO)-layer may be replaced by a complex oxide slab, or the R-layer by a complex (RO)-slab. These layers can be grouped into two blocks: the charge reservoir block (CRB) of $[(EO)(AO)_m(EO)]$ and the active block (AC) of $\{(CuO_2)[R(CuO_2)]_{n-1}\}$. The symmetry of the cuprates with the simple R-layer interleaves can vary from primitive to body-centered when m changes from an odd to an even number.
- As shown in the generic phase diagram in Fig. 3, superconductivity is induced in the cuprates from their insulating antiferromagnetic parents by hole- (or electron-, not

shown) doping and hole-doping gives rise to a higher T_c than electron-doping. Doping can be accomplished through various channels by chemical substitution, addition, or reduction; by application of pressure; by irradiation of photons; or by application of an electrical field. The most commonly used method is chemical doping in the CRB. Occasionally, chemical doping is carried out in the AB. It is believed that superconductivity takes place in the (CuO_2) -layers in the AB and that the doping process occurs in the CRB to provide carriers to the (CuO_2) -layers without introducing defects in them, similar to the modulation-doping that happens in the semiconductor quantum-well devices. Modulation-doping in cuprates retains the (CuO_2) -layer integrity that has been demonstrated to be crucial to achieving high T_c .

- As also shown in Fig. 3, the normalized T_c varies with the hole-concentration (p) according to a universal quadratic relation [12], $T_c/T_c^{\text{max}} = [1 - 82.6(p - p_0)^2]$. The compound is optimally doped when $p = p_0 \sim 0.16$ holes/Cu, where T_c peaks at T_c^{max} , underdoped when $p < p_0$, and overdoped when $p > p_0$. Cuprates in the underdoped, but not the overdoped, region display anomalies in a wide range of properties below a characteristic temperature $T^* > T_c$, suggesting the opening of the so-called pseudo-gap or spin-gap [13]. This behavior cannot be described satisfactorily by the Fermi-liquid theory. The underdoped cuprate metal is therefore considered “strange,” whereas the overdoped metal, “normal.”

- High temperature superconducting cuprates are type-II superconductors and exhibit a rather unusual behavior due to their high T_c , low carrier concentration, and layered structure. They provide a fertile ground for the study of vortex dynamics, the understanding of which will have a profound impact on high temperature superconducting technology.

1.3 Some Questions:

How does the T^ -line intersect the T_c -line in the generic T - p phase diagram? Does it stop at T_c , enter the superconducting region, or merge into the T_c -line asymptotically?*

Different scenarios will have different implications for the appearance of a quantum critical point, the appropriateness in assigning the “strange” to “normal” metal boundary and, ultimately, the occurrence of high temperature superconductivity. Unfortunately, at the present, results from different experiments appear to support different scenarios [13].

How does the anomalous behavior associated with the “strange” metal affect the appearance of high temperature superconductivity?

Suggestions have been made that the high T_c of cuprates is the consequence of the anomalous non-Fermi liquid behavior associated with the underdoped compounds [13,14]. Unfortunately, this cannot be reconciled with the fact that the overdoped compound exhibits an equally high T_c , but behaves normally above T_c , as displayed in Fig. 3.

What is the relationship between T^ and T_c ?*

Some suggest that below T^* , superconducting pairs form but phase-lock between these pairs takes place only when the temperature is lowered to below T_c . For instance, both microwave conductance and Nernst effect measurements seem to support such a suggestion [15]. However, others propose that some carriers actually localize below T^* and thus are removed from the Fermi surface, weakening the superconducting order parameter. This appears to be consistent with recent space-resolved scanning tunneling experiment observations [16] that the pseudo-gap below T^* is temperature independent and does not merge with the temperature-dependent superconducting gap below T_c . In this latter scenario, the anomalous behavior below T^* actually competes against superconductivity below T_c , similar to the competition between the martensitic transformation and the superconducting transition in the superconducting A15 or anti-ferromagnetic intermetallic compounds. We would like to point out that a similar phase

diagram exists in several intermetallic compound systems if one replaces the concentration with pressure and the T^* with the martensitic transformation or Néel temperature [17].

What is the underlying mechanism responsible for the occurrence of a pseudo-gap, and thus T^ ?*

Strong electron correlation has been proposed to be the main cause of T^* . However, a large oxygen-isotope effect has recently been observed on T^* [18], suggesting a significant role for phonons, and thus the Jahn-Teller effect, in the process. We would like to note that the oxygen-isotope effect on T^* reported is positive, *i.e.* T^* is enhanced rapidly as the isotopic mass of oxygen increases. This is similar to what has been observed on the charge order-disorder transition temperature in manganites and nickelates, where charge carriers localize below the transition temperature and form stripes, similar to that observed in the cuprates.

What is the mechanism responsible for the high T_c in cuprates?

The presence of a strong electron correlation in cuprates has been demonstrated by the existence of the insulating state of the undoped cuprates, the transfer of spectral weights

from high to low energies with doping, the small electron-phonon coupling as deduced from transport measurements, and a large Hubbard interaction. Accordingly, many models have adopted the strong electron correlation manifested by spin fluctuations as the mechanism for high temperature superconductivity [19]. Cited support includes the observations of a small isotope effect for optimally doped cuprates, and the d-wave pairing; and the previous belief that a strong electron-phonon interaction required for a $T_c > 30$'s K would trigger structural instabilities and render such a high T_c impossible. On the other hand, strong electron-phonon interaction is evidenced from ARPES, Raman, IR, and tunneling experiments. While electron-phonon interaction alone cannot account consistently for the high T_c and the many anomalous normal-state properties, a combined effect of strong electron correlation and electron-phonon interaction may be the cause. Recently, it was proposed [20] that the large electron-phonon interaction may be predominantly responsible for the high T_c and that such an effect renormalized by the strong electron correlation can account for the unusual normal- and superconducting-state properties observed. However, some of the predictions have yet to be tested experimentally.

Is two-dimensionality indispensable for high T_c ?

The great majority of models proposed to date are based on a two-dimensional electron or hole system and thus have attached great significance to the two-dimensional nature in

regard to high temperature superconductivity. This seems to be supported by recent results on the c-axis penetration depth [21], which is much greater than that predicted by the interlayer tunneling models. However, high pressure more often than not enhances the T_c and such a pressure-induced T_c -enhancement can be very large, as for the Hg-based high temperature superconductors, as pressure makes the compound more 3D-like. The cause of such a positive pressure effect remains unexplained.

What are the robustness and the role of the symmetry of the superconducting order parameter?

The symmetry of the superconducting order parameter was originally considered to be able to discern the different superconducting mechanisms. Unfortunately, the situation appears to be more complicated. While phase-sensitive experiments [22] clearly show that the superconducting order parameter has a d-symmetry, suggesting the prominent role of strong electron correlation in cuprates, renormalization of the electron-phonon interaction and the residual Coulomb repulsion were later proposed to be able to give rise to a d-wave as well. A recent tunneling experiment further shows that the symmetry can vary with doping [23]. This may imply that the two different mechanisms are in operation simultaneously, although with a doping-dependent weighting factor.

What is the effect of phase separation on high temperature superconductivity?

Phase separation that produces stripes leading to a dynamic or static inhomogeneity has been demonstrated to be a rather common phenomenon in the highly correlated electron systems of cuprates and transition metal oxides [24]. Until now, most models of high temperature superconductivity have been based on a homogeneous electron system in cuprates, although some attach great significance to the inhomogeneous nature in regard to the cause for high temperature superconductivity in the compounds. The exact role of inhomogeneity remains uncertain.

Why does the T_c depend on n , the number of CuO_2 -layers per unit formula?

The variation of the T_c of a cuprate compound with the carrier concentration p has been demonstrated to follow rather well the quadratic universal relation as described earlier (with minor modifications in some cases) when the T_c is normalized to its maximum value T_c^{max} . This implies that p is the most important parameter in determining superconductivity in cuprates and that a single CuO_2 -layer will be sufficient, rendering interlayer coupling irrelevant. However, T_c for all cuprate compound systems is found to increase initially with n for n up to 3 or 4, before it decreases with further n -increase. The drop of T_c has been attributed to the different dopings between the inner and outer layers

and the associated detrimental proximity effect on the T_c . This is because, in samples with $n > 3$, the outer CuO_2 -layers tend to be overdoped, whereas the inner layers tend to be underdoped, due to the Coulomb repulsion and charge screening [25]. As a result, the optimal T_c cannot be achieved; on the other hand, the large T_c -increase with n , at least for $n < 4$, *e.g.* 134 K for Hg1223 *vs.* 90 K for Hg1201, suggests that an additional effect in terms of electron density of states and/or an interlayer-coupling effect may be in operation.

Why do different cuprate compound systems have different T_c 's and why should a cuprate compound system that has a Ba-based charge-reservoir-block display higher T_c 's than its Sr-containing counterpart?

The rather large variation of T_c^{max} between different cuprate compound systems, *e.g.* 93 K for Cu1212 (or YBCO) but 128 K for Hg1212, is rather puzzling. Furthermore, cuprates with a Ba-containing CRB often have a higher T_c^{max} than those containing Sr, *e.g.* 108 K for Tl2212 (with a Ba-containing CRB) but 85 K for Bi2212 (with a Sr-containing CRB). This clearly demonstrates that components additional to the CuO_2 -layers are important to superconductivity in cuprates. We would like to point out that a Ba-containing ferroelectric perovskite compound usually also has a higher Curie temperature than its Sr-

containing counterpart due to the greater polarizability of the Ba-ion. It is not clear if a similar reason holds for superconductivity in cuprates.

Is a room temperature superconductor a possibility?

To date, there appears to be no theoretical or experimental reason that T_c cannot be further raised to room temperature. A wide variety of cooperative phenomena have been shown to exist in compounds with strong electron correlation. The ordering temperatures of these cooperative phenomena can be more than several hundred degrees Kelvin. Given the similarities between these compounds and cuprates, it appears that a superconductor with a T_c equal to or higher than room temperature is not an impossibility. The limit may eventually be the melting point of the compound.

Is the model simulation approach sufficient to unravel the origin of high temperature superconductivity?

Impressive success has been achieved in model simulation to obtain superconductivity with high T_c in the square-planar lattice of CuO_2 , without considering the interlayer interaction and the phonon effect and thus providing evidence for the t-J model [26]. However, it is not clear if this is a unique solution, given many of the problems posed

above. One may raise the question of whether high temperature superconductivity is an emergent phenomenon in a complex system where the conventional deductive method is no longer sufficient, similar to the case of the quantum Hall effect. In the conventional deductive approach, a theory can be constructed once the basic building blocks of the system are known.

1.4 Material Challenges

It will make the interpretation of experimental data much easier and help resolve some of the questions raised above if the following challenges can be overcome, although some may never be overcome since they may be inherent properties of the cuprates:

- **Crystallinity:** Cuprate superconductors are highly anisotropic structurally and thus electrically (as high as $\sim 10^6$) and magnetically ($\sim 10^2$). Perfect single crystals of large size are needed for crucial experiments. At present, they are available only for a few compound systems.
- **Doping uniformity:** Both the electrical and magnetic properties depend sensitively on the doping of the cuprates. However, there exists a large oxygen-diffusion anisotropy ($\sim 10^6$) between measurements along and perpendicular to the CuO_2 -plane. This,

together with the Coulomb repulsion between carriers in different CuO_2 -layers within a unit cell for large n , tends to make it difficult to obtain single-crystalline samples of size with a uniform charge distribution.

- Sample homogeneity: Both static and dynamic phase separations have been reported in some single-crystalline cuprate samples, yet many macroscopic experimental data have been explained by treating the sample as a uniform system. It may be worthwhile to determine if phase separation can be overcome.
- Chemical complexity and chemical instability: Cuprate superconductors are chemically complex and unstable. This enhances the difficulty in sample handling and characterization, especially for spectroscopy studies. Finding ways to stabilize the compounds will help alleviate the impasse.
- Compound diversity: Almost all models to date have been built on a homogeneous two-dimensional electron system in the CuO_2 -layers of the cuprates. To test the generality of these models, more diverse compounds, preferably non-cuprates or even non-oxides with equally high T_c , are needed. Unfortunately, the bismuthates, the fullerites, and the recently discovered MgB_2 have not helped much in this respect because they have relatively low T_c and behave rather similarly to the conventional

low T_c superconductors. However, experiments on the field-induced superconductivity in C_{60} and $CaCuO_2$ should provide valuable information.

- Adjustable anisotropy: This will help to test the role of dimensionality in the occurrence of high temperature superconductivity in cuprates and to improve the performance of cuprate superconductors.

2. Superconducting Ferromagnets

The layered structure of cuprates enables one to meso-material engineer the compounds for the simultaneous introduction of various collective phenomena into a unit cell of the compound. By replacing the CuO -chain layers in $GdSr_2Cu_3O_7 = CuSr_2GdCu_2O_7 = Cu1212$ by the RuO_2 -layers, one obtains the $RuSr_2GdCu_2O_8 = Ru1212$, which consists of the ferromagnetic ($SrRuO_3$)-slab superimposed on the superconducting active block that contains the CuO_2 -layer, as shown in Fig. 4. One may further replace the Gd -layer by two GdO -layers and obtain the $RuSr_2Gd_2Cu_2O_{10} = Ru1222$. Both $Ru1212$ and Ce -doped $Ru1222$ (including those with the Gd -element substituted by Eu) have indeed been found to undergo a magnetic transition at T_m and a superconducting transition at T_s with $T_m > T_s$. The transition temperatures (T_m and T_s) are (90-180 K, 15-50 K) for $Ru1212$ [27] and (122-180 K, 32-42 K) for $Ru1222$ [28]. Although an antiferromagnetic structure

associated with the Ru-sublattice was detected in Ru1212 below T_m by neutron scattering study [29], a small but unmistakable spontaneous moment has also been observed below T_m . They are therefore called superconducting ferromagnets (SCFMs), in contrast to the ferromagnetic superconductors with $T_s > T_m$ that were discovered and extensively studied in the 70's. It is known that cuprates are mainly d-wave superconductors and many display a phase separation [22,24]. SCFMs offer a unique opportunity for the study of the interaction of d-wave superconductivity with ferromagnetism and phase separation and of the influence of phase separation on magnetism in cuprate superconductors. In spite of the extensive effort in the last few years, the basic problem as to the coexistence of a uniform superconducting order and a uniform ferromagnetic order in SCFMs remains unresolved. Our study demonstrates that a non-uniform crypto-superconducting state may exist in these cuprate SCFMs. Such a superconducting state appears to consist of submicron superconducting antiferromagnetic domains separated by thin ferromagnetic boundaries, resulting from phase separation.

As shown in Fig. 5 for Ru1212, the magnetic transition is clearly evidenced by the rise in the field-cooled (FC) magnetization (M) and the anomaly in the zero-field-cooled (ZFC) magnetization at $T_m \sim 133$ K, indicating the appearance of a spontaneous moment. The superconducting transition at $T_s \sim 30$ K manifests itself in the sharp drops in the ZFC-magnetic susceptibility ($\chi \equiv M/H$) and the resistivity (ρ) on cooling. Both drops are

shifted to lower temperatures by external magnetic fields characteristic of a superconducting transition. However, the FC- χ does not show a significant diamagnetic shift, characteristic of the Meissner effect expected of a superconducting transition. A small diamagnetic drop in FC- χ has been observed in some samples at T_s and ascribed to the Meissner state [27]. Unfortunately, the drop appears only in a very small field and diminishes in a field as small as ~ 10 Oe with T_s unshifted, uncharacteristic of a Meissner effect. The observed superconducting signal has thus been attributed to one of the four possibilities [30], *i.e.* the presence of (1) a minor superconducting phase, (2) a very strong flux pinning, (3) a spontaneous vortex state, or (4) other unusual superconducting state.

As mentioned earlier, Ru1212 is derived from YSCO ($\text{YSr}_2\text{Cu}_3\text{O}_7$). Pure YSCO, which has a T_c up to 70 K depending on the oxygen-doping, cannot be synthesized at ambient pressure. However, it can be stabilized by partial Ru-substitution for Cu or by high pressure [31] and thus becomes the most likely candidate for possibility (1). To determine if a small amount of the superconducting Ru-doped YSCO is present, we have carried out a systematic study on the formation of Ru1212 and Ru1222. Polycrystalline samples have thus been prepared by the standard solid-state reaction technique at ambient pressure without any detectable impurity phase within the powder XRD resolution of a few percent. EDX analysis displayed a chemical homogeneity within a scale of ~ 1 μm and

the SEM data showed grains of dimensions $\sim 1\text{-}5\ \mu\text{m}$. The superconducting current density was determined magnetically for Ru1212 samples with different particle sizes [30], ranging from ~ 1 to $0.01\ \text{mm}$, and was found to be almost constant, as shown in Fig. 6, suggesting that the samples are electrically uniform to within $0.01\ \text{mm}$. This is consistent with the same magnetic microstructures of the sample in its remnant state due to the superconducting current at $5\ \text{K}$ and in the ferromagnetic state at $62\ \text{K}$, as determined by the magneto-optical imaging and shown in Fig. 7 [32]. These observations suggest that it is very unlikely that the superconducting signal in Ru1212 or 1222 is caused by the presence of a minor superconducting phase and thus rule out possibility (1).

For a Type-II superconductor such as the SCFMs, the flux pinning can reduce the size of the diamagnetic shift in the FC-mode and thus the Meissner signal. For a very large flux pinning, the Meissner effect may be completely suppressed. To remove the pinning effect as well as the magnetic background of Ru1212, we have determined [33] the superconducting component of the reversible magnetization (M_s) of the sample at $5\ \text{K}$ as a function of field, *i.e.* $M_s = [M_r(\text{Ru1212 at } 5\ \text{K}) - M_r(\text{Ru1212Zn at } 5\ \text{K})] - [M_r(\text{Ru1212 at } 50\ \text{K}) - M_r(\text{Ru1212Zn at } 50\ \text{K})]$, by measuring the reversible magnetization of the superconducting Ru1212 and the non-superconducting Zn-doped Ru1212 both below and above the T_c of Ru1212. The reversible magnetization $M_r \equiv (M_+ + M_-)/2$, where M_+ and

M_{\pm} are the magnetizations measured during field-increase and -decrease, respectively. The results are shown in Fig. 8, together with that for an underdoped YBCO sample with a similar transition temperature of ~ 40 K for comparison. Clearly, the diamagnetic shift of the Ru1212 is negligible and cannot be more than 1-2% of that for YBCO with a similar T_c . Therefore the negligible Meissner signal cannot be attributed to possibility (2), the presence of a large flux pinning force.

On cooling, a SCFM becomes ferromagnetic below T_m and then superconducting below T_c . As it enters the ferromagnetic state, an internal field $H_{in} = -4\pi M$ due to the spontaneous moment (M), will be generated. The internal field will be quantized and trapped inside the sample below T_c if the flux pinning is large. A spontaneous vortex state has thus been predicted [27,30]. A non-negligible superconducting condensation energy

$F_s = \int_0^{H_{c2}} M_s dH$ is expected for such a state. However, it is negligible for Ru1212 as shown

in Fig. 8, not more than a few percent of that for the underdoped YBCO in the presence

of a field $\sim H_{in}$, *i.e.* $\int_{H_{in}}^{H_{c2}} M_s dH$. Consequently, the absence of a Meissner signal is unlikely

to be due to possibility (3), the presence of a spontaneous state.

Therefore, a novel crypto-superconducting state was advanced to account for the absence of the Meissner state [30,33]. It must be non-uniform in nature with superconducting domains much smaller than the crystal grains revealed by the SEM analysis, and smaller than the penetration depth. If this is the case, there should be more than one superconducting transition for the domain, the inter-domain, and the inter-grain, respectively, with the first as the bulk and the others as phase-lock transitions. A closer examination of the magnetic and resistive data indeed reveals multiple superconducting transitions as local peaks at ~ 30 and 40 K, shown in Fig. 9. Two different length scales also reveal themselves in the particle size (d) effect on the real part of the ac magnetic susceptibility (χ') [34], as displayed in Fig, 10. The magnitude of χ' below ~ 30 K decreases rapidly with d -decrease even for $d > 20 \mu\text{m}$. On the other hand, the magnitude of χ' between ~ 30 and 40 K does not change with d -decrease until $d < 10 \mu\text{m}$. A penetration depth of $\sim 0.64 \mu\text{m}$ is obtained by analyzing the data. By examining the magnitude of χ' , which represents the superconducting condensate, it is concluded that the peak at 40 K cannot correspond to a bulk of Ru1212 but to a phase-lock transition between domains similar to that at 30 K between grains. To determine the magnetic characteristics of the domains, a thermo-magneto-hysteretic effect study was made [35] on a diluted sample of Ru1222 particles of $\sim 1 \mu\text{m}$ smaller than the crystalline grain size of $2\text{-}10 \mu\text{m}$. An unusual, but universal memory effect across T_m was observed. The data

suggest that domains with a FM component, a “precursor” of the T_m -transition, already exist far above T_m and that the memory effect is due to the demagnetization field of these “precursor”-domains. The relative space-correlation between the “precursor”-domains and the domains of the T_m species, therefore, can be estimated. Our analysis suggests that the Ru1222 samples are predominantly antiferromagnetic and the ferromagnetism component below T_m must be small in terms of volume fraction, resulting from phase separation, which is common in underdoped cuprates. These antiferromagnetic domains are expected to be superconducting below T_c since their coexistence has previously been demonstrated.

Therefore, we have demonstrated that there exists a novel non-uniform crypto-superconducting state in the so-called SCFMs, where superconductivity coexists with the antiferromagnetic domains of scale $< 0.3 \mu\text{m}$, separated by ferromagnetic boundaries resulting from phase separation. In addition to the yet-to-be-determined bulk transition of Ru1212 above 40 K, we have identified a grain-grain phase-lock transition at 30 K and a domain-domain transition at 40 K. The T_c 's of Ru1212 previously reported by various groups are basically the grain-grain phase-lock transition temperature. A grain-grain phase-lock transition temperature depends sensitively on the coupling between grains. The crypto-superconducting state proposed above explains the large variation of the reported T_c in pure samples by different labs and the very field-sensitive small

diamagnetic shift detected in Ru1212 and 1222. With the proposed presence of ferromagnetic boundaries between small superconducting domains, these compounds may provide a unique opportunity for spin polarization study on the sub-micron scale.

3. Multi-Wall Carbon Nanotubes in Magnetic Fields

Carbon nanotubes have attracted great attention in the last several years because of their interesting unusual physical properties and nano-device potential. They are in the forms of multi-wall nanotubes (MWNTs) with a typical diameter of 5-30 nm and single-wall nanotubes (SWNTs) of a smaller 0.4-2 nm diameter. Nanotubes are considered to be ideal model systems to test theories on the transport as well as magnetic properties of low-dimensional systems. Both ballistic and diffusive transport, and metallic and semiconducting behavior have been predicted, depending on the dimension, helicity, and doping of the nanotubes. Indeed, experimental observations often can be explained by the theories and in other cases can confirm some of the theoretical predictions. Various device functions have also been demonstrated in both SWNTs and MWNTs. They include ballistic conducting wires, field effect transistors, single electron transistors, rectifiers, and spin electronics. Since magnetic fields can alter the electronic structure of the nanotubes, unusual properties have also been predicted in nanotubes in the presence of magnetic fields. However, studies on the magnetic properties of nanotubes in magnetic

fields are sparse in comparison with those on the transport properties, and most were done in earlier days when the samples were not well characterized.

Strong electron correlation has been suggested for carbon nanotubes where a Luttinger liquid state has been proposed. In a one-dimensional system such as SWNTs, one expects collective low-lying excitations, but with no long-range order. Recently, superconducting behavior dominated by fluctuations was reported by Tang *et al.* [11] in uncoupled 4 Å SWNTs below 20 K with an estimated mean-field transition temperature of 15 K. On the other hand, a sharp resistivity drop of two orders of magnitudes, signaling the occurrence of a superconducting transition at 0.55 K, has been reported by Kociak *et al.* [36] in ropes of coupled SWNTs. In the hope of detecting superconductivity at a higher temperature by suppressing fluctuations *via* inter-wall coupling, we have examined the magnetic and electrical properties of MWNTs in the presence of magnetic fields, although the electron-phonon interaction is known to decrease with an increase in the diameter of the nanotubes, such as MWNTs.

The MWNTs investigated were prepared by an arc process from high purity graphite (SES Research, Houston, Texas). The tubes have a length 2000-5000 nm and consist of 5-20 layers of graphite with a diameter of 1.2-20 nm. The samples were ropes of MWNTs of dimensions of 0.1x1 mm. The magnetic susceptibility χ was measured both

in the FC and ZFC modes between 5 and 400 K in fields up to 5 T. The difference between the FC and ZFC- χ is small. The results of the FC- χ are summarized in Fig. 11, where the FC- χ of graphite is also included for comparison. In zero field, χ of MWNTs is relatively large and negative at 400 K. This is in contrast to the χ of C₆₀, which is slightly paramagnetic and almost temperature-independent. It becomes progressively more diamagnetic as temperature decreases with a negative curvature above ~ 100 K and a positive curvature below. In other words, χ displays an “S-shape” temperature dependence. When a magnetic field is applied, χ changes very little above 300 K but becomes less diamagnetic below 300 K. The resistance (R) of the MWNT ropes was measured up to 325 K in fields up to 5 T and the results are summarized in Fig. 12. The sample is rather conducting with a resistivity of $\sim 10^{-3}$ Ωcm comparable with published data. At zero field, R behaves as a semiconductor and increases monotonically with temperature decrease. In the presence of a magnetic field, R at high temperature increases rapidly, *e.g.* $\sim 52\%$ at 325 K in 5 T. However, at lower temperatures, the field-induced R-increase slows down. All R(T)-curves in a field 2 T or higher exhibit a slightly reduced slope near 100 K and cross the zero field R(T) around 60 K. Such an inflection point in R(T), *i.e.* the temperature where dR/dT has a local maximum, is shifted upward by field as shown in the same figure. The origin is not clear.

While nanotubes are expected to become more graphite-like as the diameter increases, the zero-field χ of the MWNTs at 300 K is only $\sim 20\%$ that of the graphite. This may be ascribed to the presence of distorted carbon hexagons in MWNTs. However, the large temperature dependence of χ makes it more diamagnetic than graphite below ~ 30 K as also shown in Fig. 11. Such a strong temperature dependent χ of MWNTs is indeed unusual, not to mention its stronger field dependence than for graphite [37]. The χ does not fit the $1/T$ dependence predicted by the band-effect. The “S-shape” temperature-dependent χ is reminiscent of the opening of a spin-gap (Δ) that often takes place in a low-dimensional system [38]. The model predicts $\chi = a + b \exp(-\Delta/kT)$, with a , b , and Δ as the fitting parameters. As shown by the solid curves in Fig. 11, it describes well the experimental data at different fields above ~ 50 K but gives more positive values than the measured results below ~ 50 K. The deduced value of Δ increases from 5.88 to 15.76 meV as the field increases from 1 to 5 T. The physical meaning is unclear. The “S-shape” T-dependence of χ of MWNTs looks like a broad superconducting transition with an inflection point occurring near 100 K and the small diamagnetic signal may be ascribed to the small MWNT diameter in comparison with the penetration depth. The magnetic field effect on the χ of MWNTs observed is consistent with that of a superconductor, although the small but positive field-effect on the inflection point temperature of χ , where $d\chi/dT = 0$, is a puzzle.

The resistivity of our MWNT rope samples behaves as a semiconductor, where a negative magnetoresistance usually is expected. On the contrary, a large positive magnetoresistance was observed, at least above ~ 50 K. This may be explained in terms of a mixture of metal and semiconductor. Since undoped and perfect MWNTs are expected to be metallic, the semiconducting behavior may be attributed to defected sections of the tubes or contacts between tubes that are much shorter than the sample length. It is known that the transport properties of a metal/semiconductor mixed system are usually overwhelmed by the semiconducting component, giving rise to the overall semiconducting behavior of MWNTs, especially at low temperatures. The magnetoresistance of a semiconductor is large and negative in general. This may account for the negative magnetoresistance observed below ~ 50 K. The magnetoresistance of a metal with a large mean free path such as pure Mg usually is positive and large. However, this picture may not be applicable to the MWNT samples studied because of their relatively large resistivity. The large positive magnetoresistance observed in MWNTs may be understood in terms of a mixture of semiconductor and metal, if one assumes that the metallic component is superconducting at temperature as high as 300 K. However, the negligible field effect on χ at 300 K poses a serious challenge to such an explanation. On the other hand, one may attribute the small field effect on χ to the small

superconducting component of χ of MWNTs due to the large penetration depth in comparison with their small diameter. At lower temperatures, inter-tube coupling enhances the apparent diameter of the MWNT samples and thus the superconducting component of χ , which becomes field effective below ~ 200 K, as shown in Fig. 11.

In conclusion, unusual field effects on the transport and magnetic properties have been observed in MWNTs. The reason is unknown. Although some of the observations may be superconducting-like, the suggestion of superconductivity at very high temperature is rather speculative at the present and needs further investigation. If superconductivity is indeed eventually proven to exist in these interesting materials, it may be a non-conventional type where the large diamagnetism is associated with the persistent current of the large molecular orbitals of the MWNTs. If this is true, the flux quantum will be h/e instead of the $h/2e$ for a conventional superconductor.

4. Comments on the Recent Paper “Possible superconductivity above 400 K in carbon-based multiwall nanotubes” by Guomeng Zhao and Y. S. Wang

By extending our results described above, Zhao and Wang [39] in our lab recently made the claim as described in the title of the paper based mainly on: (1) a very large field

effect on the diamagnetic χ at low field, *i.e.* a four-fold increase at 5 K from 20 mG to 0.28 mG; (2) a large positive moment in the remnant state after the withdrawal of a strong field of 5 T and its decay with temperature; and (3) a resistance rise starting at ~ 600 K and extending to ~ 750 K, the highest temperature of the experiment. Because of the potential significance of the claim, both careful examination of the original raw data (with the consent of Wang) and new experiments were done to check these databases. Unfortunately, the results so obtained demonstrated that the bases were faulty and the claim cannot be substantiated. The current status concerning the unusual electrical and magnetic properties remains the same as described earlier in this article and there is no evidence of superconductivity above 400 K, as claimed. Reasons are described below:

It is known that because of field trapping by the superconducting magnet in the SQUID magnetometer used for the experiment, extreme care has to be taken for low-field quantitative measurements, especially below 1 Oe. Using superconducting Pb in its Meissner state as an *in situ* field sensor for very low field measurements, the M of MWNT samples from the same batch was found to vary with field linearly without hysteresis up to 1.5 Oe. Therefore no field-effect on χ was detected at low fields between 0.05 and 1.5 Oe. However, in one sample a negative M-intercept appeared at 0 Oe, due to a minute amount of magnetic impurity present, since the intercept became positive when the sample orientation was physically reversed. The magnetic impurity induced by non-

zero negative apparent M at very low field can mistakenly be taken to give rise to a large field-dependent χ as stated in (1).

Indeed, a large positive M , which decayed with temperature-increase, was detected in samples from the same MWNT batch, used by Zhao and Wang, in their remnant state following the same procedure as Zhao and Wang. However, the M of this sample was carefully measured as a function of field and clearly exhibited an unambiguous negative curvature at low field, characteristic of the presence of a magnetic impurity. The application and subsequent withdrawal of a high field in the process of creating the remnant state aligns the spins of the magnetic impurity and makes the detection of negative curvature much easier as compared with a virgin sample. The analysis of the original raw data obtained by Zhao and Wang showed the same magnetic signature. Therefore, the positive remnant moment is magnetic but not superconducting in nature, as stated in (2).

The R-anomaly reported was not reproducible from sample to sample and through thermal cycling. Zhao and Wang extrapolated the R between 300 and 600 K to 750 K as the superconducting background R and attributed the difference (ΔR) as that caused by the proposed superconducting-to-normal transition above ~ 600 K. The field-induced R-

increase at 395 K and 5 T happened to be about the same as ΔR . This was cited as a proof for the superconducting transition, although no field-induced R-saturation was in sight. Additionally, such a suggestion implies that the alleged superconducting transition above ~ 600 K will be completely pushed to below 395 K by a field of 5 T and the R below 359 K at fields lower than 5 T is independent of field. This is in complete contradiction to the large positive magnetoresistance even down to 150 K as shown in Fig. 12. Therefore, basis (3) is both intrinsically and extrinsically flawed.

5. Field-Induced Superconductivity—A Comment

The reported field-induced superconductivity (FIS) [4,9,10] up to 117 K in pure and intercalated C_{60} , pure C_{70} , $CaCuO_2$, and $[CaCu_2O_3]_4$ is one of the most exciting advancements in the study of high temperature superconductivity in recent years. The technique using a gate-voltage to inject carriers into the material of interest goes far beyond the study of superconductivity. It provides a new tool for the study of materials, although restricted to the surface layers. An excellent talk has been presented by Bertrum Batlogg at this Symposium. Among the exciting results reported by Batlogg are: (1) The T_c varies with carrier concentration following the universal relation $T_c(p)$, although with different maximum T_c 's for different materials and different signs of the carrier charge; (2) a T_c of 117 K in intercalated C_{60} is close to that of the maximum T_c of 134 K in

cuprates; (3) the $T_c(p)$ of FIS in electron-doped C_{60} is the same as that for the chemically doped bulk C_{60} ; (4) the $T_c(p)$ of the hole-doped FIS in $CaCuO_2$ is the same as that for the chemically doped bulk cuprates; (5) FIS is proposed to occur in the first layer of the materials examined; and (6) the perfection of the surface of the materials is considered to be crucial for FIS.

While confirmation of these experiments is yet to be made, I would like to offer a few comments concerning the implication of these experiments for the occurrence of high temperature superconductivity in cuprates in the following:

- (1) The non-monotonic universal $T_c(p)$ that is independent of materials suggests that a two-dimensional electron or hole system is sufficient to sustain high temperature superconductivity, supporting the 2D argument for layered cuprates. However, the similar T_c observed in the 2D FIS in C_{60} and the chemically doped 3D C_{60} implies that dimensionality may not be so crucial. If FIS is indeed 2D, we would like to raise the interesting question of whether it is associated with the long-sought-after exciton-mediated surface superconductivity at the metal/semiconductor interface that was first proposed by Allender, Bray, and Bardeen in 1973 [40]. The FET device arrangement may provide the ideal condition to meet the stringent requirements for the occurrence of surface superconductivity of this type, *i.e.* the close coupling between the metal

and the semiconductor, the sharpness of (or no chemical reaction at) the metal/semiconductor interface, and the matching of the Fermi levels of the metal and the semiconductor.

- (2) The similar maximum T_c of FIS in the non-magnetic C_{60} and the magnetic cuprates insinuates that spins are not necessary for high temperature superconductivity, in contrast with many models for cuprates where magnetic origin has been assumed.

- (3) A sample with a perfect surface has been emphasized to achieve FIS, since defects on the surface create defect states that tend to localize the carriers. However, it is known that the infinite-layer cuprate $CaCuO_2$ -films are usually loaded with defects, since they are not grown under an equilibrium condition. The reported high T_c in this compound therefore poses the question of whether a perfect surface is necessary for FIS. If not, one may ask if superconductivity is indeed confined to the surface. Although calculations indicate that the carriers should reside only in the top molecular layer of the sample, the rather sharp superconducting transition observed does not seem to be characteristic of a 2D transition that is dominated by fluctuations.

- (4) The observation of FIS in $CaCuO_2$ -films has also suggested that the apical oxygen may not be needed for the occurrence of superconductivity in cuprates in contrast to a

previous conjecture [41]. However, it was recently pointed out [42] that the oxygen atoms in the gated Al_2O_3 -layers and the Cu ions in the CaCuO_2 -layers may form five fold coordinated Cu^{+2} ions with apical oxygens.

FIS has opened up new opportunities and has raised many questions in our study of high temperature superconductivity in the bulk and on the surface as well. Much more excitement is expected to come.

6. Acknowledgment

I would like to thank my collaborators, Y. Y. Xue, R. L. Meng, B. Lorenz, Y. S. Wang, J. Cmaidalka, Y. Y. Sun, and J. Lenzi for their hard work and helpful discussions. Special thanks go to Y. Y. Xue for his critical review of the manuscript and numerous suggestions. The work in Houston is supported in part by NSF Grant No. DMR-9804325, the T. L. L. Temple Foundation, the John J. and Rebecca Moores Endowment, and the State of Texas through the Texas Center for Superconductivity at the University of Houston; and at Lawrence Berkeley Laboratory by the Director, Office of Science, Office of Basic Energy Sciences, Division of Materials Sciences and Engineering of the U.S. Department of Energy under Contract No. DE-AC03-76SF00098.

7. References

1. For example, Takagi, H., *Physica C* **341-348**, 3 (2000); Müller, K. A., *ibid*, 11 (2000); Kitazawa, K., *ibid*, 19 (2000); Chu, C. W., *ibid*, 25 (2000); Rice, T. M., *ibid*, 41 (2000).
2. Bednorz, J. B. and Müller, K. A., *Z. Phys. B* **64**, 189 (1986); Wu, M. K. *et al.*, *Phys. Rev. Lett.* **58**, 408 (1987); Cava, R. J. *et al.*, *Nature* **232**, 814 (1988).
3. Haddon, R. C. *et al.*, *Nature* **350**, 320 (1991).
4. Schön, J. H., Kloc, Ch. and Battlog, B., *Nature* **406**, 702 (2000); Schön, J. H. *et al.*, *Science* **288**, 656 (2000).
5. Schilling, A. *et al.*, *Nature* **363**, 56 (1993).
6. Chu, C. W. *et al.*, *Nature* **363**, 323 (1993); Gao, L. *et al.*, *Phys. Rev. B* **50**, 4260 (1994).
7. Chu, C. W. *et al.*, *Science* **277**, 1081 (1997).
8. Nagamatsu, J. *et al.*, *Nature* **410**, 63 (2001).
9. Schön, J. H., Kloc, Ch. and Battlog, B., *Nature* **414**, 434 (2001).
10. Schön, J. H. *et al.*, *Science* **293**, 2432 (2001).
11. Tang, Z. K. *et al.*, *Science* **292**, 2462 (2001).
12. Presland, M. R. *et al.*, *Physica C* **176**, 95 (1991).

13. Timusk, T. and Statt, B., Rep. Progr. Phys. **62**, 61 (1999); Tallon, J. L. and Loram, J. W., cond-mat/0005063; Loktev, V. M. *et al.*, cond-mat/0012082.
14. For example, Emery, V. J. and Kivelson, S. A., Nature **374**, 434 (1995); Anderson, P. W., Nature **279**, 1196 (1998).
15. Xu, Z. A. *et al.*, Nature **406**, 486 (2000).
16. Suzuki, M. and Watanabe, T., Phys. Rev. Lett. **85**, 4787 (2000); Krasov, V. M. *et al.*, Phys Rev. Lett. **86**, 2657 (2001).
17. Bilbro, G. and McMillan, W. L., Phys. Rev. B **14**, 1887 (1976); Chu, C. W. and Diatchenko, V., Phys. Rev. Lett. **41**, 572 (1978); Mathur, N. D. *et al.*, Nature **394**, 39 (1998).
18. Temprano, D. R. *et al.*, Phys. Rev. Lett. **84**, 1990 (2000).
19. For example, P. Monthoux, P. and Pines, D., Phys. Rev. B **47**, 6069 (1993).
20. For example, Kuli, M. L., Phys. Rep. **338**, 1 (2000).
21. Kirtley, J. R. *et al.*, Phys. Rev. Lett. **81**, 2140 (1998).
22. For a review, Tsuei, C. C. and Kirtley, J. R., Rev. Mod. Phys. **76**, 969 (2000). It should be noted that R. A. Klemm *et al.* pointed out that the order parameter symmetry could also be determined by examining the c-axis twist-angle (Φ) of the twist-boundary critical current density (J_c) in a junction or an array of uniform junctions. Q. Li *et al.* subsequently found a Φ -independent J_c and thus suggested that the order parameter in BSCCO should have the s-symmetry. However, the issue of

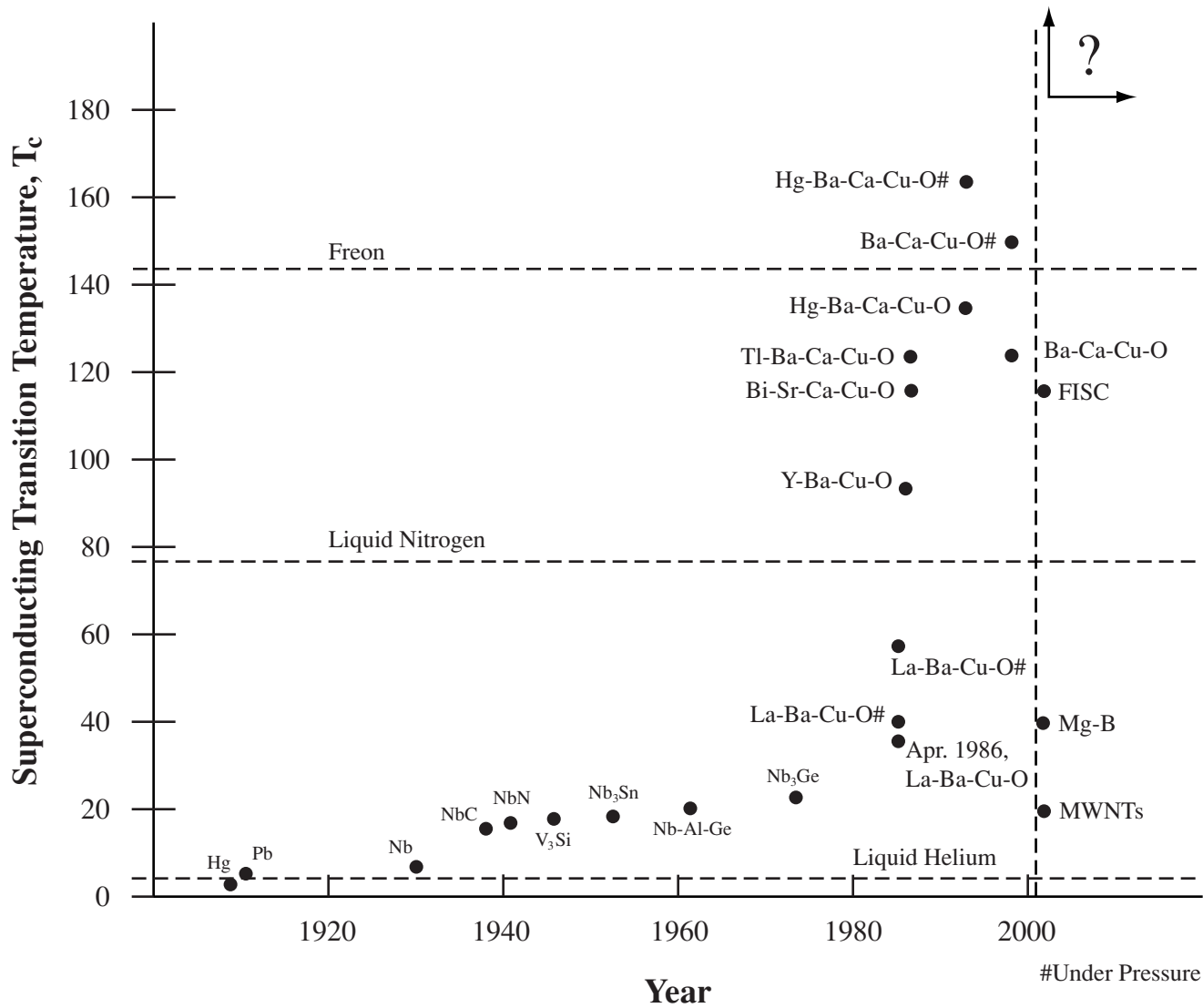
- uniformity of the junctions in the microscopic BSCCO sample examined remains unresolved [Phys. Rev. Lett. **83**, 4160 (1999)].
23. Yeh, N. C. *et al.*, Phys. Rev. Lett. **87**, 087003 (2001).
 24. For example, Tranquada, J. M. *et al.*, Nature **375**, 561 (1995); Moreo, A., Yunoki, S. and Dagotto, E., Science **283**, 2034 (1999).
 25. Di Stasio, M., Müller, K. A. and Pietronero, L., Phys. Rev. Lett. **64**, 2827 (1990); Lin, Q. M., PhD Thesis, University of Houston, 1996.
 26. Scalapino, D. J., Phys. Rep. **250**, 329 (1995); Kampf, A. P., *ibid* **249**, 220 (1994).
 27. Bernhard, C. *et al.*, Phys. Rev. B **59**, 14099 (1999); Bernhard, C. *et al.*, Phys. Rev. B **61**, 14960 (2000); Meng, R. L., Physica C **353**, 195 (2001).
 28. Felner, I. *et al.*, Phys. Rev. B **55**, 3374 (1997).
 29. Lynn, J. W. *et al.*, Phys. Rev. B **61**, 14964 (2000).
 30. Chu, C. W. *et al.*, Physica C **335**, 231 (2000).
 31. Xiong, Q. *et al.*, Physica C **198**, 70 (1992); Cao, Y. *et al.*, Phys. Rev. B **58**, 11201 (1998).
 32. Chen, S. Y. *et al.*, cond-mat/0105510.
 33. Xue, Y. Y. *et al.*, Physica C **341-348**, 459 (2000).
 34. Xue, Y. Y. *et al.*, Physica C **341-348**, 483 (2000); Xue, Y. Y. *et al.*, Physica C **364-365**, 251 (2001).
 35. Xue, Y. Y. *et al.*, cond-mat/0109500.

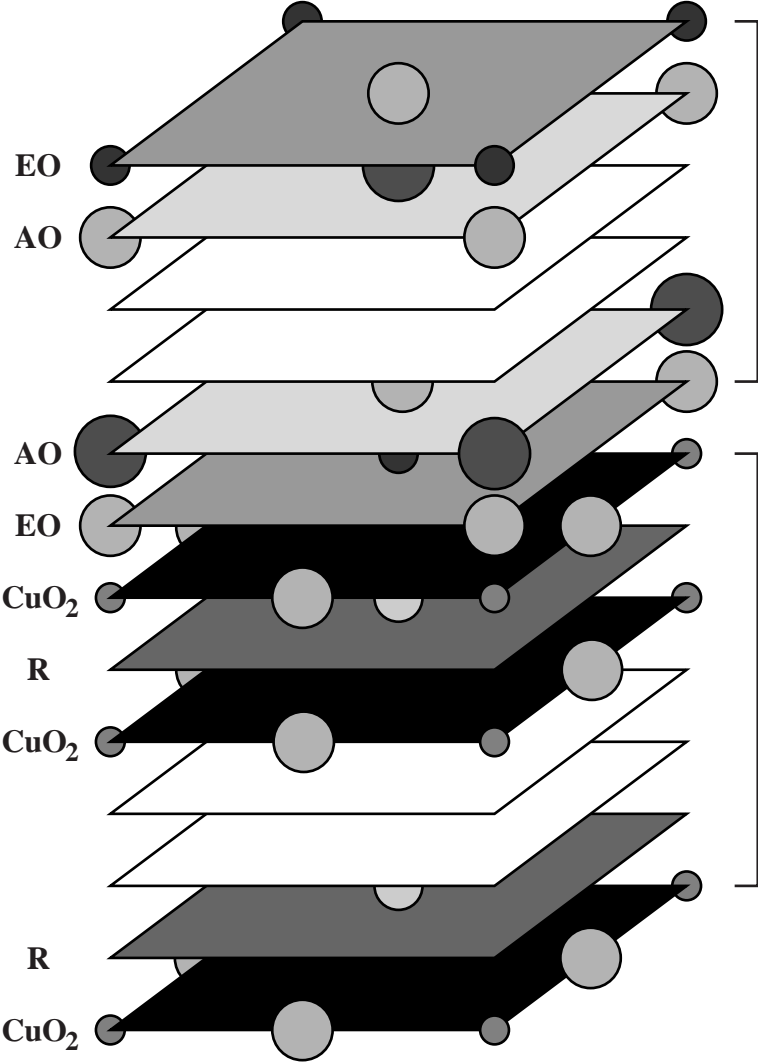
36. Kociak, M. *et al.*, Phys. Rev. Lett. **86**, 2416 (2001).
37. For example, Nicholls, J. T., McNiff, E. J. and Dresselhaus, G., Phys. Rev B **42**, 5555 (1990).
38. For example, Johnston, D. C. *et al.*, Phys. Rev. B **61**, 9558 (2000).
39. Zhao, G. M. and Wang, Y. S., cond-mat/0111268.
40. Allender, D., Bray, J. and Bardeen, J., Phys. Rev. B **7**, 1020 (1973).
41. Nücker, N. *et al.* J. Supercond. **12**, 143 (1999).
42. Müller, K. A. and Chu, C. W., cond-mat/0203457.

8. Figure Captions

- Fig. 1: T_c vs. time.
- Fig. 2: A schematic structure of cuprate superconductors.
- Fig. 3: The generic phase diagram of cuprates.
- Fig. 4: The structures of Ru1212 and YBa₂Cu₃O₇.
- Fig. 5: a) FC (top curve) and ZFC (lower curve) M/H's of Ru1212. Inset: ZFC-M/H in an expanded scale near the transition. b) ρ of the same sample at different H's.
- Fig. 6: The width of the M-H loops (\square) and the J_c (\blacktriangle) of Ru1212 powders with different particle sizes at 5 K.

- Fig. 7: The magneto-optical images of a Ru1222 ceramic sample at 5 K and 62 K.
- Fig. 8: The M_s of three Ru1212 samples (●, ■, and ▲) and a YBCO sample (□). The dashed line represents the effective internal field of Ru1212, as estimated from the magnetization of the Ru1212 sample.
- Fig. 9: a) dp/dT at zero external field. b) ZFC magnetization at 5Oe for a Ru1212 ceramic sample.
- Fig. 10: The ac χ' of Ru1212 powders from the same bulk ceramic. ◇: 0.3 μm ; ▽: 0.8 μm ; △: 1.5 μm ; □: 3 μm ; and ○: 8 μm . Inset: That of powders with size of 3 mm (○); 40 μm (□); 2.3 μm (△); and 0.3 μm (▽).
- Fig. 11. The susceptibility of a MWNT sample at 1 (○), 2 (▽), 3 (□), 4 (◇), and 5 T (△). Also included is the susceptibility of graphite at 0 T (●). The lines are fits described in text.
- Fig. 12. R of a MWNT rope under the field of 0, 1, 2, 3, 4, and 5 T from the bottom to the top at high temperatures. Inset: dR/dT of a MWNT rope under the field of 0, 1, 2, 3, 4, and 5 T from the bottom to the top at low temperatures.





charge reservoir block
 $(EO)(AO)_m(EO)$

A – Bi, Tl, Pb, Cu... (AO)

E – Ca, Sr, Ba

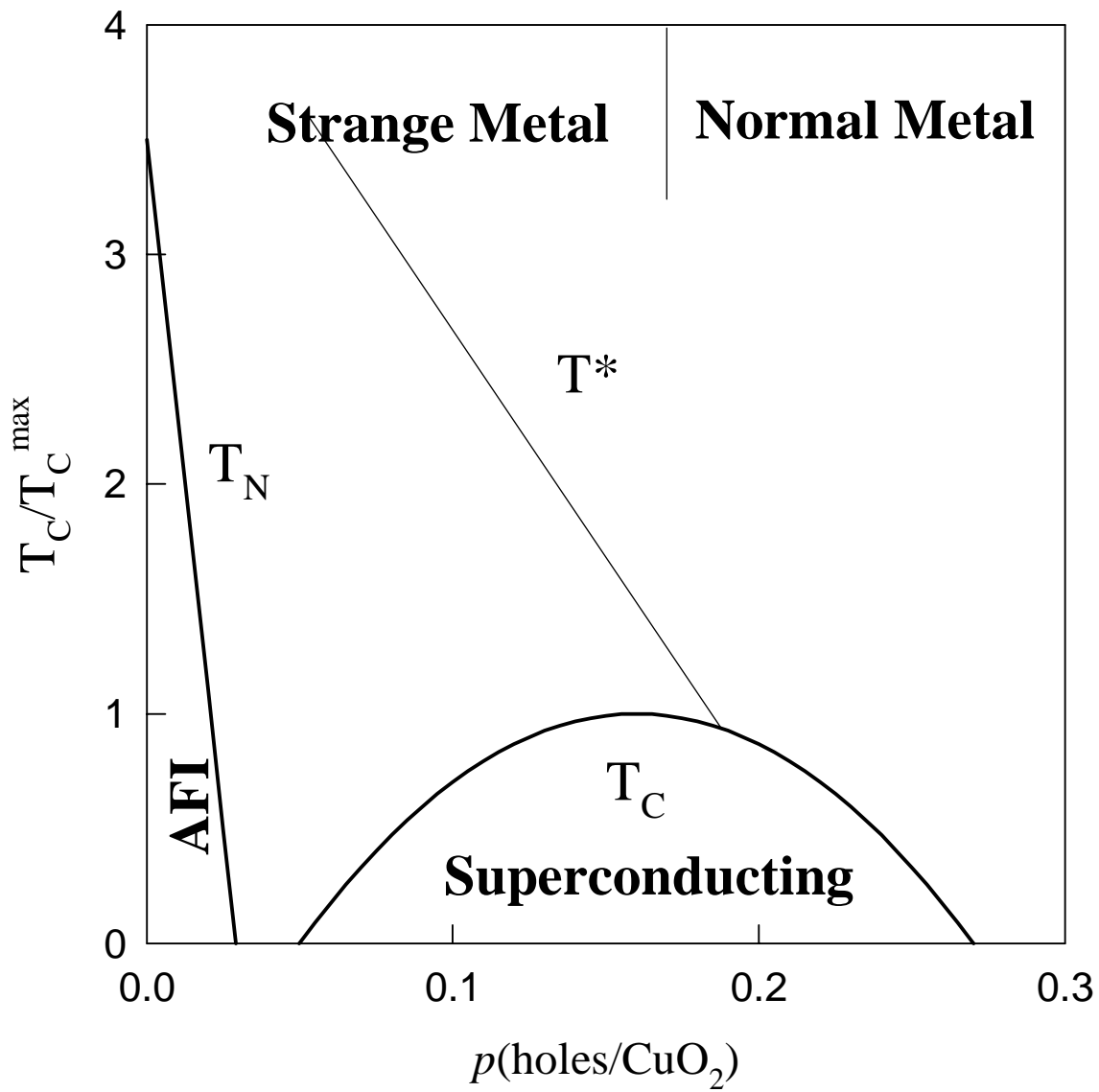
R – Ca, RE, (REO)

active block
 $(CuO_2)[(R)(CuO_2)]_{n-1}$

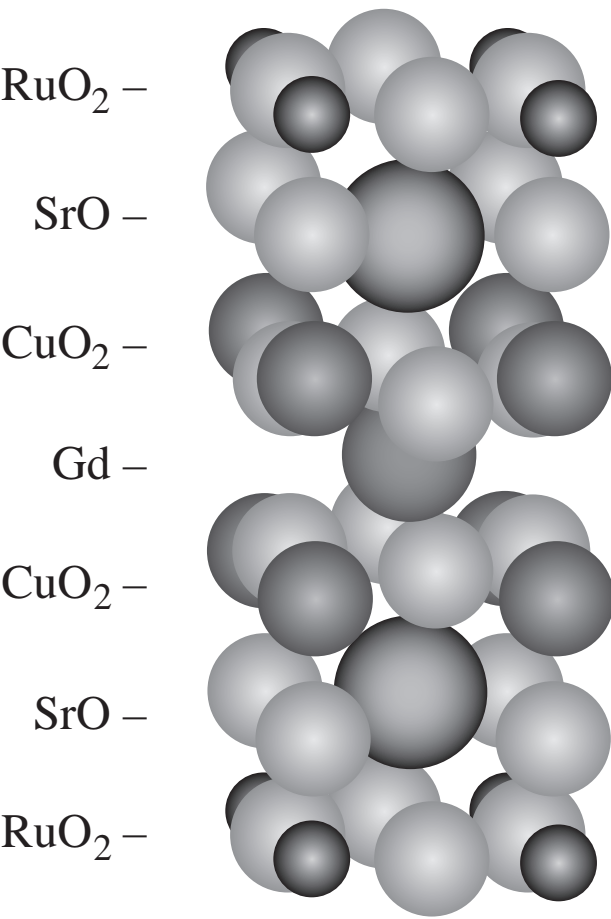
e.g. YBa₂Cu₃O₇

= CuBa₂YCu₂O₇

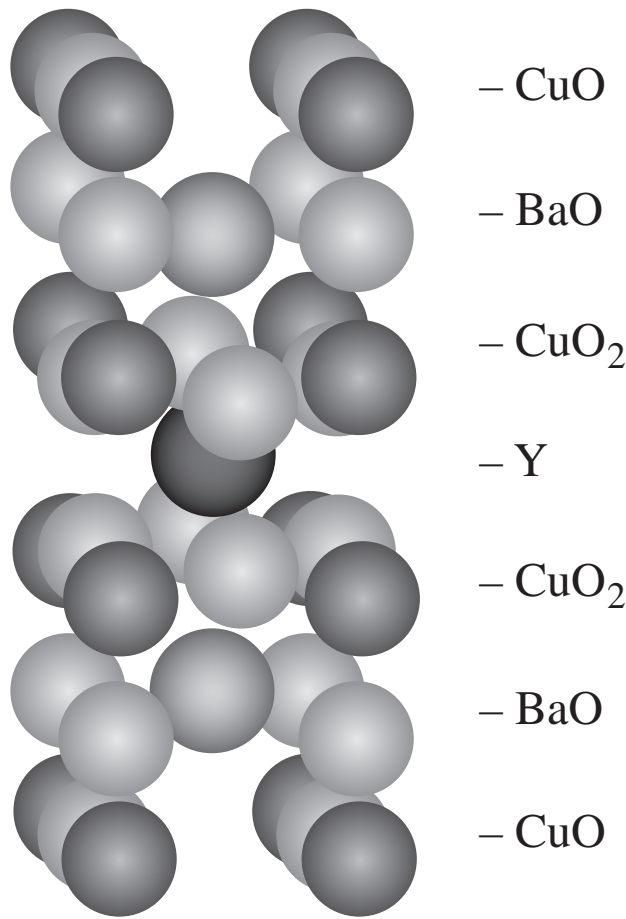
= Cu1212

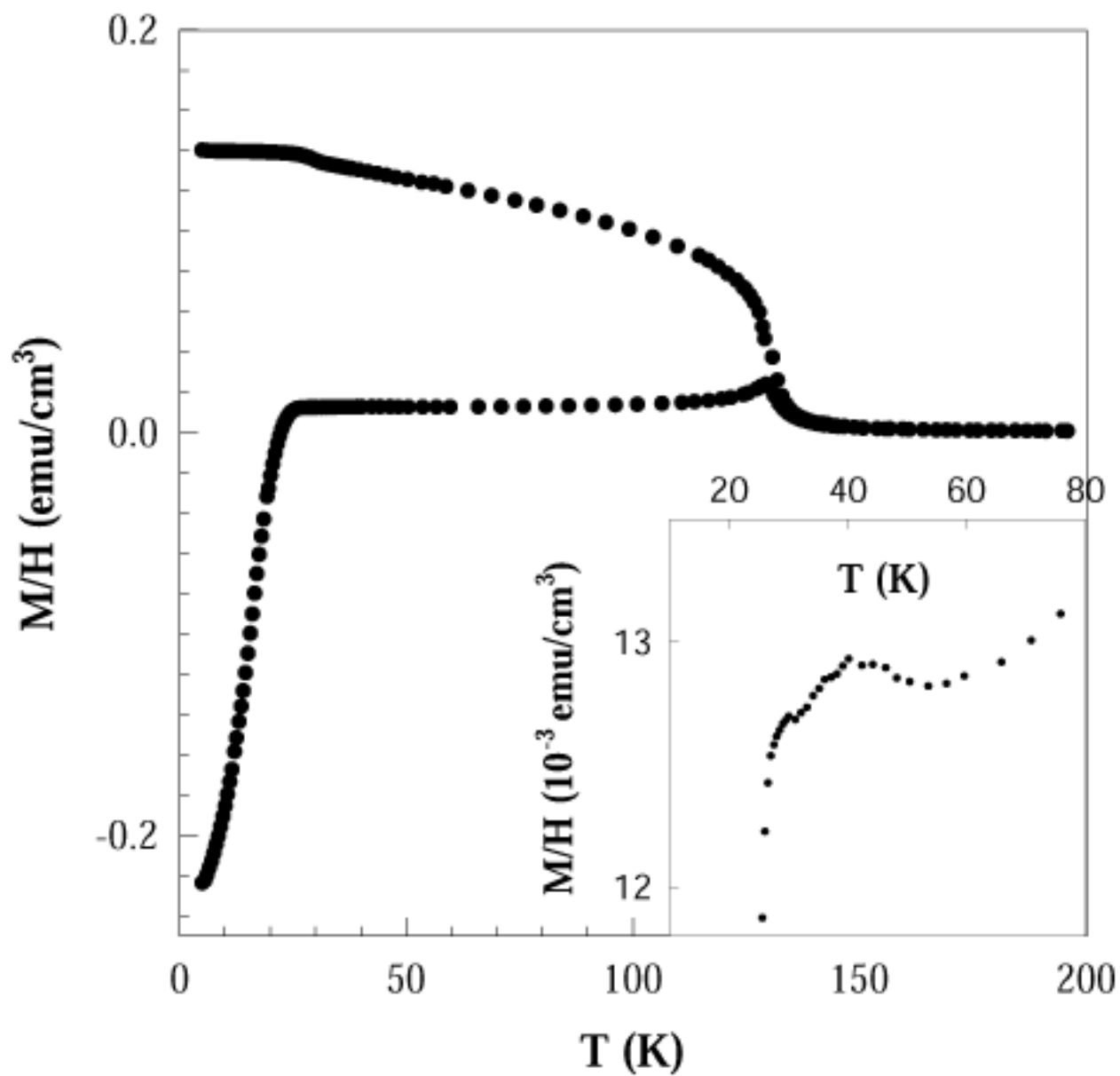


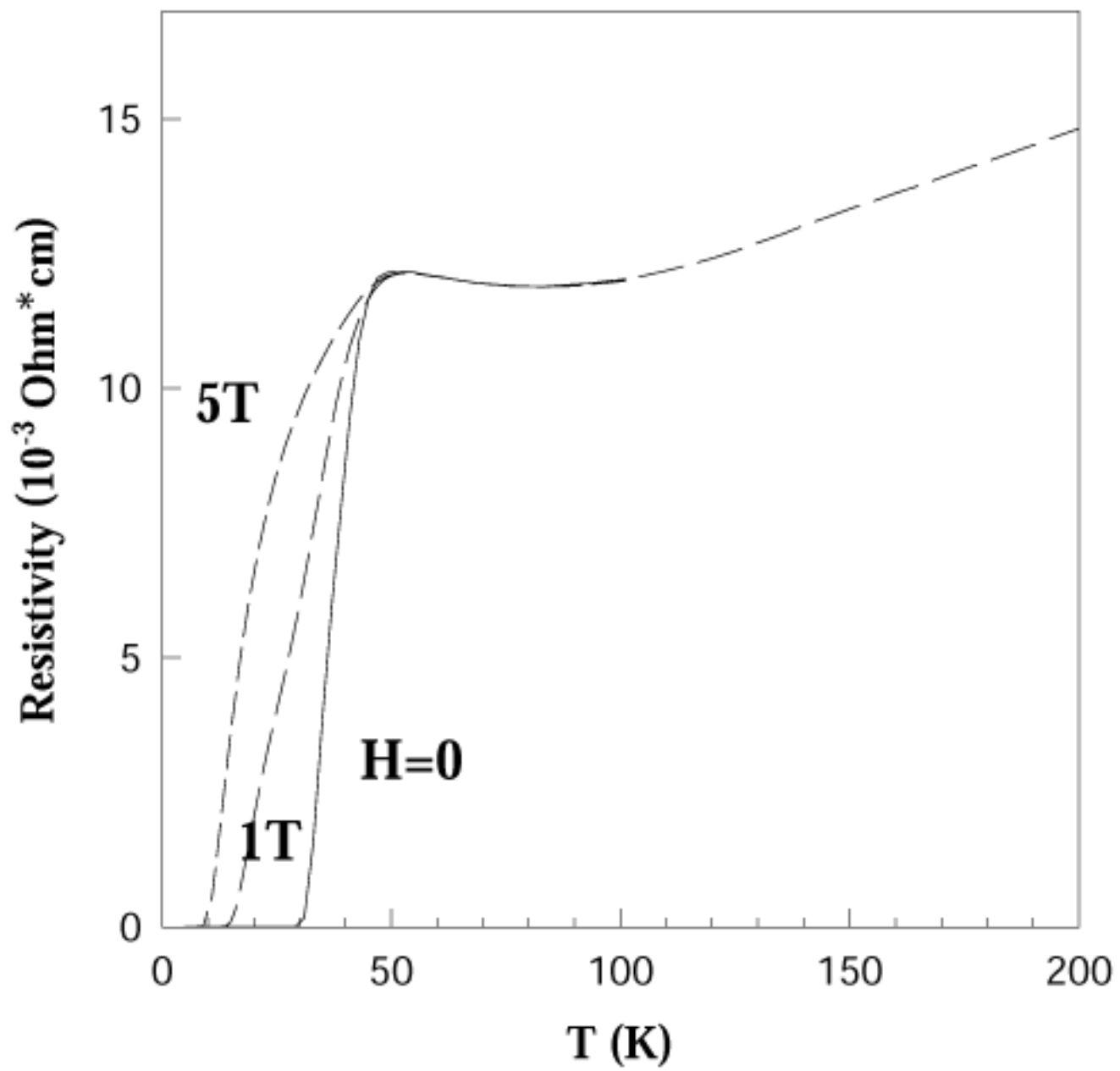
Ru-1212

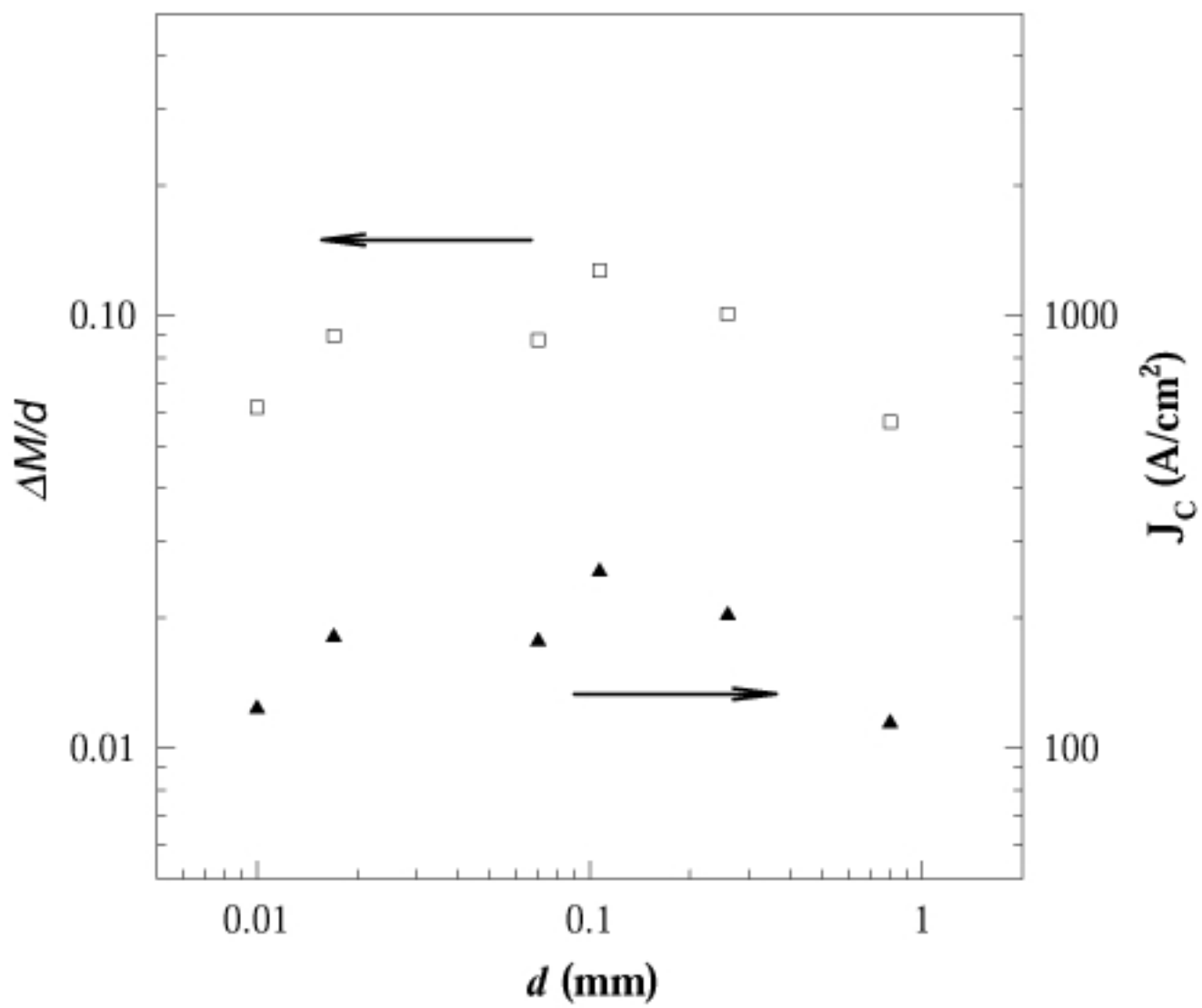


YBCO



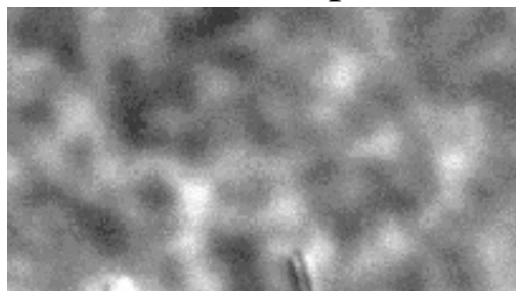






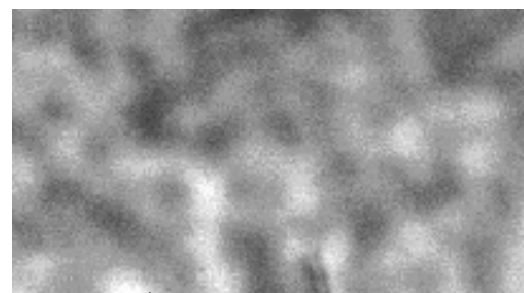
at 5 K

(FM domains+Supercurrents)



at 62 K

(FM domains only)



50 μm



